A comparison of structural analyses procedures for earthquake-resistant design of building

Latifi, Reza; Hadzima-Nyarko, Marijana

Source / Izvornik: **Earthquakes and structures, 2021, 20, 531 - 542**

Journal article, Published version
Rad u časopisu, Objavljena verzija rada (izdavačev PDF)

https://doi.org/10.12989/eas.2021.20.5.531

Permanent link / Trajna poveznica: https://urn.nsk.hr/urn:nbn:hr:133:709545

Earthquakes and Structures, *Vol. 20, No. 5 (2021) 531-542*
DOI: https://doi.org/10.12989/eas.2021.20.5.531

A comparison of structural analyses procedures for earthquake-resistant design of buildings

Reza Latifi[1a] and Marijana Hadzima-Nyarko*[2]

[1]*Civil Engineering, University of Bologna, 40136, Italy*
[2]*University J. J. Strossmayer of Osijek, Faculty of Civil Engineering and Architecture Osijek, Vladimira Preloga 3, 31000 Osijek*

(Received January 22, 2021, Revised March 30, 2021, Accepted April 5, 2021)

Abstract. Several seismic analysis procedures in the latest standards have been developed for structural design and assessment. Since these methods have different advantages and limitations, a comprehensive comparison of these procedures is required to select the most effective one. The three most common methods are the Equivalent Lateral Force (ELF) method, Modal Response Spectrum (MRS) analysis, and Linear Response History (LRH) analysis. This research intends to present a comparative study of these methods, according to ASCE 7-16 standard by utilizing ETABS® software. They were examined in terms of base shear and distribution of story shear forces for a sixth-story reinforced concrete (RC) building, designed according to ACI 318-19 standard. Building code requirements for RC structures with the dual lateral force-resisting system in a high seismic zone are discussed. The results show that the ELF procedure's base shear for the building under consideration is conservative compared to the MRS or LRH analysis. The vertical distribution of the ELF procedure is just a function of the structure's fundamental period; however, the advantage of the MRS and LRH analysis is that they provide information as to how the distribution of mass and stiffness of a structure influences the member forces and displacements.

Keywords: seismic analysis; equivalent lateral force; modal response spectrum analysis; linear response history analysis; story drift

1. Introduction

Research into the nature of earthquakes and the behavior of structures exposed to seismic actions can be considered a primary goal in seismic engineering. The behavior of reinforced concrete (RC) structures under seismic action is often the subject of consideration and research, especially in seismically active zones (Vintzileou *et al.* 2004, Günay *et al.* 2009, Ademović *et al.* 2020, Isik *et al.* 2020). The justification of interests is based on the complexity of their behavior and the fact that reinforced concrete structures are very common (Da Luo *et al.* 2019, Ghaemian *et al.* 2020).

The analyses of seismic wave propagation inside structures have been employed in recent years by several researchers for structural health monitoring, analysis of building response, and system identification (Snieder and Safak 2006, Rahmani and Todorovska 2013, 2015, Trifunac *et al.* 2010, Bulajic *et al*. 2020).

The level of complexity and detail of a building modelling method for determining the dynamic behavior of the structure exposed to dynamic loads, like earthquakes, strong winds, explosions, etc. depends on the structure complexity and the aim of the analysis (Bilgin and Uruçi2018, Hadzima-Nyarko *et al.* 2019).

Early engineering provisions for seismic analysis and earthquake resistance of buildings were made at the beginning of the twentieth century (Strukar *et al.* 2019). For example, in the United States, the Uniform Building Code (UBC) was first published in 1927 with the concept of equivalent static analysis with seismic coefficient varied between 7.5% and 10% of the total building's gravity plus live load. In 1957, the Modal Response Spectrum (MRS) analysis was developed for the first time. The structure's energy dissipation was considered in 1959. The performance-based seismic design philosophy introduced in 1967 by SEAOC Blue Book was a significant transition from traditional structural design and intends that a structure reliably reaches the desired likely performance objectives during a given earthquake. Applied Technology Council (ATC) regulations, ATC 3-06, were released in 1978 and organized most modern seismic analysis principles. The key difference from conventional design for gravity is greater ductility for high seismicity regions meaning that the structure can withstand large deformations without failing (Fajfar 2018).

Nonlinear Static Procedure (NSP) or Pushover Analysis was first introduced in the 1970s, and it got the name Capacity Spectrum Method (CSM) in the 1980s. This is a graphical procedure that compares the structure's capacity with seismic demands. The CSM in ATC 40 standard was used for seismic evaluation and retrofit of concrete buildings in 1996. In FEMA 273 (1997), the target displacement was defined by the coefficient method in 1997. The first standard to include Nonlinear Dynamic

*Corresponding author, Associate Professor
E-mail: mhadzima@gfos.hr
[a]M.Sc.
E-mail: rlatifi1983@gmail.com

ISSN: 2092-7614 (Print), 2092-7622 (Online)

Table 1 Comparison of different analysis methods and limitations

Analysis procedure	Equilibrium Equations	Structural irregularity	High inelastic demand	Higher mode effects	Near source earthquakes
LSP	$Ku = F$	×	×	×	×
LDP	$M\ddot{u}(t) + C\dot{u}(t) + Ku(t) = F(t)$	✓	×	✓	×
NSP	$Ku + F_{NL} = F$	✓	✓	×	×
NDP	$M\ddot{u}(t) + C\dot{u}(t) + Ku(t) + F(t)_{NL} = F(t)$	✓	✓	✓	✓

Procedure (NDP) in design work was UBC in 1991. The seismic structural response is characterized by substantial uncertainties concerning ground motion and structural modeling so that an explicit probabilistic procedure would be suitable. In 2012, the ATC developed FEMA P-58 with a framework for performance-based earthquake engineering based on research developments of Cornell and Krawinkler. The method for performance-based procedures is defined by Section 1.3 of ASCE 7-10 and ASCE 7-16. Although codes permit these explicit probabilistic approaches, the implementations are not straightforward for most engineers.

Different analysis procedures are introduced by ASCE 7-16 (2017) to estimate the seismic demand, and recognizing their accuracy levels is still a question for researchers and engineers. The Linear Static Procedure (LSP), also known as the Equivalent Lateral Force (ELF) method, is a static analysis method with no variable lateral triangular loading pattern that simulates the seismic force to a structure that remains elastic and linear during the analysis with an unrealistic, linear force-displacement curve. It is implicitly assumed that the structure sustains damage during a large seismic event and considers the inelasticity and reduction of stiffness by Behavior Factor in an approximate way. After linear elastic analysis, the action forces or demands are compared with the members' capacities by calculating the Demand over Capacity ratio (DCR), and the structure is safe if DCR < 1. The LSP assumes that the structure vibrates according to the fundamental mode and cannot model higher mode effects and structures equipped with dampers.

Linear Dynamic Procedure (LDP) consists of two methods: the MRS and LRH analysis and in both the elasticity rules utilized, and there is no stiffness degradation during the analysis. The nonlinear behavior is assumed in the Behavior Factor's linear elastic analysis and reduction of RC structural members' stiffnesses. In the MRS procedure, the lateral forces' profile is not arbitrary and is computed as a combination of the structure's different modes' modal contributions. In RHA, the earthquake record is applied at the building base, and structural behavior, story drifts, and member forces are monitored. Dynamic equilibrium equations are solved using either modal or direct-integration methods. The structural members' action effects in terms of forces are compared with the capacities, and if DCR < 1, the structure is safe.

In the NSP, the structural behavior is no longer linear, either in conventional or adaptive mode. Stresses, forces, and bending moments are not proportional to strains, displacements, and curvatures, respectively. Different lateral force profiles such as uniform, triangular, modal, or adaptive distributions that change in each step could be utilized. As the plastic hinges develop in each step, the structure gradually softens, and the member stiffness is reduced and updated. The monotonic force-displacement curves should be introduced for sections that are expected to respond inelastically. Such effects cannot be captured accurately by the LSP. In the NDP, the structural response is nonlinear and inelastic, and forces are not proportional to deformations. The hysteretic behavior of seismic-force-resisting elements that are expected to experience damage to design ground motions needs to be modeled.

In general, nonlinear analysis has not been well standardized for the design process, it is too complicated and time-consuming for conventional use and is, also, not convenient for practicing engineers (Head *et al*. 2014). Therefore, the present study tries to shed light on the linear analysis procedures presented in ASCE 7-16 (2017), which applies to new structures. Table 1 compares analysis methodologies with their equilibrium equations. Notations M, C, K, and F are the mass, damping, stiffness, and force matrix, respectively. Matrices of dynamic analysis denoted by `t` and may vary with time.

According to modern seismic design standards, buildings require proper consideration in detailing the sections where plastic hinges are supposed to occur. Infill walls and staircases also affect reinforced concrete (RC) buildings' seismic response and should be modeled if they significantly contribute to the seismic response.

Moehle *et al.* (1986) studied the RC structures response having irregular vertical configurations subjected to earthquake simulations on a shaking table. They found that dynamic and inelastic static methods were superior to the elastic methods in evaluating structural discontinuities' effects. Chopra (2017) implemented the MRS and LRH approach for the five-story shear frame. The MRS method's peak base shear estimated by Square Root of the Sum of the Squares (SRSS) or Complete Quadratic Combination (CQC) rules is smaller than the RHA values by about 10%. It was about 15% for the top-story shear since the higher modes' responses are most significant relative to the first mode. Charney *et al.* (2020) investigated an 8-story steel building's structural response located in Raleigh Hills, Oregon, utilizing ELF, MRS, and LRH procedures. Their case study building was designed according to AISC 2016b with perimeter steel special moment-resisting frames in one direction, and dual braced frame-moment frames in an orthogonal direction. Their results indicate considerable scatter in the computed base shears for the different analysis methods. Aswegan and Charney (2014) performed four different analysis cases for a four-story steel special

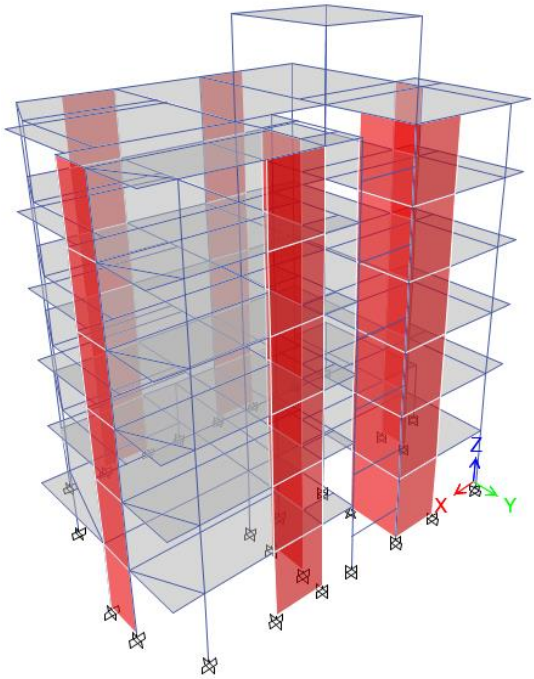

Fig. 1 3D view of RC building

moment frame building, and the results are compared. Their results illustrated that three spectral matched LRH cases produce base shears approximately 94% of MRS methods' base shear using the ASCE 7-10 response spectrum. Inter-story drift ratios are an average of 100% of the MRS inter-story drift ratios.

Following chapter 19 of ASCE 7-16, soil-structure interaction (SSI) effects can be considered when analyzing seismic design forces and the structure's corresponding displacements. SSI effects are not considered in this research.

From this short overview, it can be seen that several seismic analysis procedures in the latest standards have been developed for structural design and assessment. Since they have different advantages and limitations, this research intends to present a comparative study of the three most common methods, the Equivalent Lateral Force (ELF) method, Modal Response Spectrum (MRS) analysis, and Linear Response History (LRH) analysis, in order to obtain the most effective one. They were examined in terms of base shear and distribution of story shear forces for a reinforced concrete (RC) building.

2. Model description

A six-story residential RC building was analyzed and designed according to the ASCE 7-16 and ACI 318-19 regulations for structures located in a high seismic zone, and the relative accuracy of different linear seismic analyses is compared. The building's seismic force-resisting system in two orthogonal directions consists of combining the RC shear wall and moment-resisting frame. The first-floor height is 3.3 m, and the typical story height above the first story is 3.2 m. The integrated software package for the structural analysis and design of buildings ETABS® (2019) was used to carry out the work presented in this research. The 7th floor refers to an attic above the staircase shown in the three-dimensional finite element model of Fig. 1. The building's plan, dimensions, and structural member's geometry consist of beams, columns, and shear walls are shown in Fig. 2. The cross-section dimensions are assumed to be constant, although they could be reduced along with the height as the seismic demands decrease. The concrete modulus of elasticity and mass per unit volume is assumed to be 2766 kgf/mm^2 and 2500 kg/m^3, respectively. The steel modulus of elasticity and mass per unit volume is assumed to be 20389 kgf/mm^2 and 7849 kg/m^3, respectively.

Section 2.3 of ASCE 7-16 presents five basic gravity load combinations and two load combinations with seismic load effects. Uniformly distributed Dead Load (DL) and Live Load (LL) applied to the in-plane rigid diaphragms. The DL and LL floor 1 to 5 are 540 and 200 kgf/m^2, respectively. The DL, LL, and Snow Load (SN) for the roof is 470, 150, and 110 kgf/m^2. The effect of vertical ground acceleration may be considered using additional vertical forces on the balcony's cantilever beams, i.e., 0.2DL. Structural components and foundation must have strength equals or exceeds the envelope (most critical) of these load combinations. Those types of loads that may develop inertial forces during an earthquake should be included in the seismic analysis since base shear is produced from the accumulated inertial forces over the structure's height, which is so-called Effective Seismic Weight, i.e., DL+0.2LL. Due to stiffness and mass deviations in design, construction, and loading from the idealized case, the locations of the centers of rigidity and mass for a floor typically cannot be determined with a high degree of accuracy. Hence, code requires considering a minimum eccentricity of 5% of a structure's width in each direction (Heausler 2015). The mass offset from the stiffness center tends to couple the lateral and torsional modes. Seismic and wind loads need not be considered to act simultaneously.

According to Section 11.4 of ASCE 7-16, an elastic spectrum is used for the linear RHA's target spectrum and the MRS approach. ATC Hazard Tool was utilized to determine the ground motion parameters in specific geographical locations. For site latitude-longitude coordinates of (45, −122), Risk Category of II, and Site Class of C, useful ground motion parameters are presented in Table 2. After specifying ground motion parameters for the location, the elastic response spectrum is plotted with four branches using Eqs. (1) to (4) as illustrated in Table 2. The transitional periods are T_0=0.2T_S and T_S=S_{D1}/S_{DS}. The long-period transition periods (T_L) could be extracted from the standard's figures or the ATC's web-based tool. According to Section 12.6, using the ELF method is limited to structures with height and period lower than 48.8m and 3.5T_S, respectively. The elastic spectrum is presented in Fig. 3.

According to Section 1.5 of the standard, buildings must be classified based on the risk to human life and welfare associated with their damage or failure by their occupancy or use. The Redundancy factor (ρ) addresses the need for

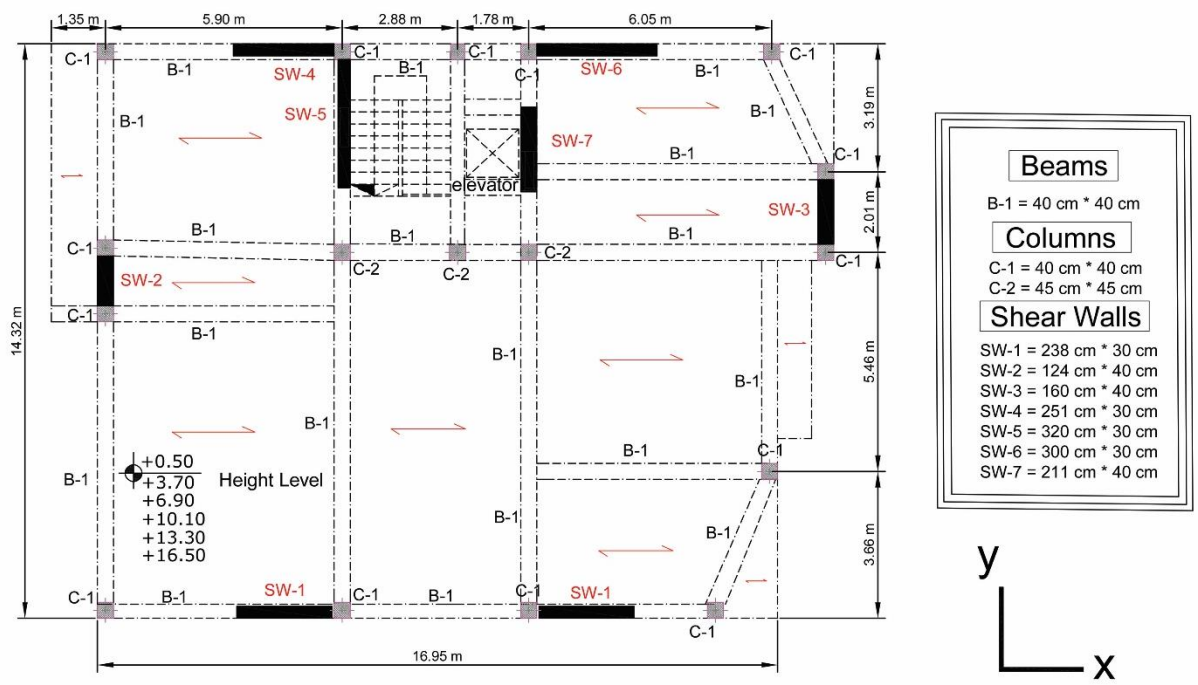

Fig. 2 Six-story building plan

Table 2 Details of Elastic Response Spectrum Branches based on the Ground Motion Parameters

Ground Motion Parameters		Elastic Response Spectrum Branches		
Seismic design category (SDC)	D	$T < T_0$	$S_a = S_{DS}\left(0.4 + 0.6\frac{T}{T_0}\right)$	(1)
MCE$_G$ peak ground acceleration (PGA)	0.296			
Numeric seismic design value at 1.0s SA (S_{D1})	0.262	Const. accel., $T_0 < T < T_S$	$S_a = S_{DS}$	(2)
Numeric seismic design value at 0.2s SA (S_{DS})	0.467	Const. vel., $T_S < T < T_L$	$S_a = \frac{S_{D1}}{T}$	(3)
Transition period (T_S= S_{D1}/ S_{DS})	0.561	Const. displ., $T > T_L$	$S_a = \frac{S_{D1}T_L}{T^2}$	(4)
Long-period transition period (s) (T_L)	16			

multiple lateral force-resisting load paths and could be either 1.0 or 1.3 and depends on the SDC and structural configuration. The building under consideration is classified as Risk Category II, with a seismic Importance Factor (I_e) of 1.2 and has a particular arrangement of seismic force-resisting elements to qualify for ρ = 1.0. According to Section 12.2, dual systems consist of Special Moment Frames (SMF) and RC shear walls, design coefficients are R=7, Ω_0 = 2.5, and C_d = 5.5. The code requires that the moment frame must have the capacity to resist at least 25% of the total base shear, to provide a secondary seismic force-resisting system with greater redundancy degrees and ductility to improve the building's ability to carry the service loads after strong earthquake shaking. The primary structural system, namely walls or bracings, acting together with the moment frame, must resist 100% of the seismic design forces.

2.1 Structural modeling

Structural modeling, analysis, and design were carried out with ETABS software version 19. Beams and columns are modeled as line elements connected at joints, and structural analysis based on the joint-to-joint geometry may overestimate deflections. The modeling is done with rigid or semi-rigid end offsets to model member's cross-sectional dimensions and beam-column joints rigidity. Elastic elements can be used to model elements that are not expected to sustain severe damage during an earthquake, such as columns (Latifi and Rouhi 2020). The base of the building is modeled fixed with joints translation and rotation restraint. Large openings at the ground level to create free space for shop or car parking create a weak soft-story, increasing the building's vulnerability and short-span beams or columns, leading to a significant increase in shear forces brittle failure.

Flexural stiffness (EI) modifier is used in RC structural modeling to consider cracking and nonlinear behavior of members and has a significant effect on drift and second-order effects (P.D) (Wong *et al.* 2017, Shehu *et al.* 2019). The effective EI in beams decreases by increasing the applied flexural bending moment; however, it depends on the effect of axial force-bending moment interaction in columns. Section 6.6 suggests that the EI modifier for Serviceability Limit State (SLS) should be 1.4 times for the Ultimate Limit State (ULS). According to Section 6.6 of ACI 318-19 and CSA A23.3-14 (2014) standard for the ULS design of RC beams, columns, and flat slabs, EI should be reduced by factors 0.35, 0.7, and 0.25, respectively, and the EI reduction factor for shear walls

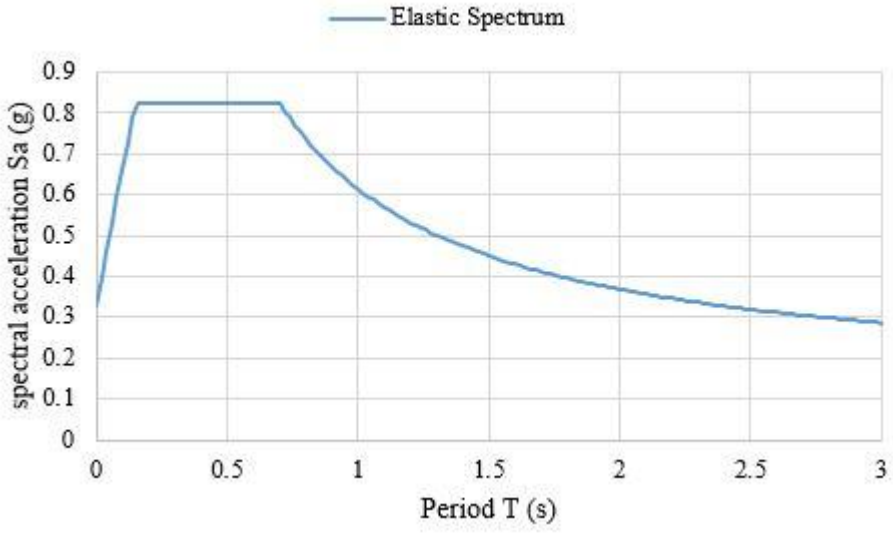

Fig. 3 Response spectrum utilized for the MRS analysis

varies between 0.35 and 0.7, depending on concrete's tensile stress. Also, Eurocode 8 and Section 6.6 of ACI 318-19 allow considering 0.5 for the EI modifier of all structural members in ULS design. EI modifiers in the New Zealand code (2006) for RC beams are 0.4, and RC columns are 0.4, 0.55, and 0.8 for low, medium, and high axial force, respectively, so as axial pressure increases, the EI modifier increases. In ETABS, the out-of-plane and in-plane stiffness of shell element used for shear walls are assumed to be 0.1, and 0.35 respectively.

Elastic shear walls are modeled with four nodes of bidirectional shell or plate elements and subdivided into a mesh of smaller rectangular or triangular elements for increasing accuracy (Reddy 2017). The main difference between thin and thick shell formulation is transverse shear deformation (Timoshenko 1959). The thin-plate formulation neglects transverse shear deformation and follows Kirchhoff's assumptions or so-called Classical Plate Theory (CPT), while the thick-plate formulation does account for shear behavior and follows Mindlin (1951) and Reissner (1945). In ETABS, Piers and Spandrels label should be assigned to shell elements for shear walls' reinforcement design. Floor diaphragms of the building under consideration are modeled as rigid. Diaphragms have flexural (out-of-plane) and axial (in-plane) stiffness and are responsible for resisting gravity loads and transmitting seismic force through their main components to the beams, columns, shear walls, or braces (Moehle *et al*. 2010). The diaphragm's in-plane rigidity determines how lateral forces will be distributed to the seismic-force-resisting elements (Ghosh 2016).

If non-structural elements interact with the structural elements and affect the response, strength, stiffness, and modal shapes, their contribution should be considered in the modeling. For example, stairs may act like a diagonal brace and damage the structure if rigidly connected to adjacent floors so, stairs may be detailed by a sliding connection on one floor and a fixed connection on another floor to allow the movement for maximum possible drift. If shear walls substantially increased lateral stiffness and strength, the stairs' rigidity does not significantly affect the structural stiffness and may not need to model stairs (Li and Mosalam 2013). The asymmetric arrangement of infill walls in plan and elevation greatly influences the structures' capacity, stiffness, and response (FEMA E-74 2012).

2.2 Analysis procedures

According to the ELF procedure, the structure is assumed to be a single-degree-of-freedom system with 100% mass participation in the fundamental mode. It follows prescriptive rules to include the inelastic dynamic response allowed only for structures without significant irregularities in mass and discontinuities in stiffness over the height. Based on Eqs. (5) and (6), the ELF base shear, V, computes from the effective seismic weight, W, multiplied by the seismic response coefficient, C_s modified by behavior factor, R, and Importance factor, I_e, to account for inelastic behavior and structural performance. The mathematical structural model's period must not exceed the empirical fundamental period, Ta, times the upper limit coefficient, C_u, as it is shown in Eq. (7). Eq. (8) derived from the lower bound estimate (mean minus one standard deviation) of the T_a for different structure types and height resulted in an upper-bond estimate or conservative total base shear, V.

$$V = \mathrm{C_s}W \tag{5}$$

$$C_s = \frac{\mathrm{S_{DS}}}{(\mathrm{R}/I_e)} = \frac{0.467}{(7/1.2)} = 0.08 \tag{6}$$

$$T = C_u T_a = 1.5 \times 0.44 = 0.66 \tag{7}$$

$$T_a = C_t h_n^x = 0.0488 \times 19^{0.75} = 0.44\mathrm{s} \tag{8}$$

The LDP includes two analysis approaches, namely, the MRS and the LRH technique. The MRS method employs peak modal responses calculated from a mathematical

Table 3 Unmatched ground motion records

Event	Station	Year	RSN	Magnitude	$D_{5\text{-}75}$ (s)	$D_{5\text{-}95}$ (s)	I_A (m/s)	R_{jb} (km)	R_{rup} (km)	V_{s30} (m/s)
Hector Mine, US	Hector	1999	1787	7.13	7.6	11.7	1.9	10.35	11.66	726
Kobe, JP	Shin-Osaka	1995	1116	6.9	4.5	11.6	0.8	19.14	19.15	256
Kocaeli, TU	Duzce	1999	1158	7.51	6.1	11.8	1.3	13.6	15.37	281.86

model's eigenvalue analysis, and modal responses are combined using SRSS or CQC to estimate total building response quantities. Only significantly contributing modes to the response require to be considered with 100%±30% rule combination (Latifi and Rouhi 2020). According to the MRS procedure of Section 12.9, the mathematical structural model is decomposed into a multi-degree-of-freedom system to determine how the actual distribution of stiffness and mass influences the elastic displacements and element forces. Assigning in-plane rigid diaphragm restraints for the building's roof reduces the number of modes (mass degrees of freedom) to two translations and one rotation per story. The elastic spectrum does not include the terms I_e and R, so it should be divided by R to accounts for inelastic behavior and multiplied by I_e to account for the additional strength required to develop essential structures' performance. To compute inelastic displacements when the elastic response dspectrum is used, C_d must amplify elastic displacements. The LRH approach means a time-step by time-step evaluation of structure response, using discretized artificial or real earthquake records as base acceleration.

According to Section 12.9 of the standard, the required number of modes to use in the LRH analysis and the force and displacement results' scaling is similar for the MRS method. The LRH analysis requires at least three pairs of scaled response histories in two orthogonal directions. The result's envelope (most critical) obtained from three ground motions is taken for the structural design (Haselton *et al.* 2017). An identical elastic response spectrum with a 0.05 damping ratio was utilized for both the MRS and LRH frequency content modification, commonly known as spectral matching, consisting of modifying each horizontal component's frequency content. The factors R, I_e, and C_d, should be applied to the LRH analysis results and note that the C_d factor captures the structural system's inelastic behavior and conservatively may be set equal to R (Uang and Maarouf 1994).

A set of 3 different far-field earthquake records and stations in the United States, Italy, and Turkey have been selected and used in this research. Each set of records consists of three orthogonal (two horizontal and one vertical) components of ground motions that are downloadable from the Pacific Earthquake Engineering Research (PEER) center's Next Generation Attenuation Ground Motions (NGA) database. Earthquake records are identified with a Record Sequence Number (RSN). The earthquake ground motion can be characterized by various parameters with particular feature such as the significant durations (i.e., $D_{5\text{-}75}$ and $D_{5\text{-}95}$), the closest distance to the rupture surface (i.e., Joyner-Boore distance (R_{jb})), the closest distance to the rupture plane (R_{rup}), average shear-wave velocity for upper 30m depth (V_{s30}) based on travel time from the surface to a depth of 30 m, and Arias Intensity (I_A) as illustrated in Table 3 (Stewart *et al.* 2011).

I_A is a ground motion parameter representing an earthquake's potential destructiveness as the integral of the square of the acceleration time history. Shear-wave velocity is a crucial parameter for estimating the dynamic properties of soils. Shear-wave velocity is a crucial parameter for estimating soils' dynamic properties and is used in the ASCE 7 standard to separate sites into different classes.

Arturo Arias, in 1970 initially developed I_A to quantify the intensity and destructiveness of earthquake shaking on buildings, which is the integral of the square of the acceleration time history and is a function of the frequency content and ground motion duration. The time history of the normalized Arias intensity, referred to as a Husid plot, is sometimes used to define the significant duration of strong shaking ($D_{5\text{-}75}$ and $D_{5\text{-}95}$), which is for the time interval between 5% to 75% or 95%. V_{s30} is a parameter to characterize site response as implemented in building standards.

For the LRH procedure, ground motion selection and modification requirements are provided in Section 12.9 of ASCE 7-16 with less detailing concerning the NDP requirements of Section 16.2. For this study, the ground motions were chosen from the far-field records presented in FEMA P-695 (2009, Appendix A, part A.9). Two horizontal components of unmatched ground acceleration in x- versus y-direction are plotted in (a), (b), and (c) of Fig. 4(d) represents the target spectrum used for the MRS and LRH analysis and three pairs of unmatched ground motion spectra. In plots (a), (b), and (c), it can be observed that X- versus Y- ground acceleration trajectories are not highly correlated, indicating that the earthquake ground motions in one compass direction are not dominant.

There are three ways to modify original time histories to match a design spectrum (Hancock *et al.* 2006). The frequency-domain matching is the nonuniform scaling of ground motion so that the acceleration response spectrum approximately matches a target (design) spectrum. In amplitude scaling, a uniform scale factor is applied to the ground motion. Time-domain spectral matching is the most commonly used technique that consists of the wavelet algorithm to adjust an original or artificial ground motion to a specific target response spectrum (Abrahamson 1992, Al Atik and Abrahamson 2010). The principal advantage of spectral matching compared to amplitude scaling is that fewer ground motions can be used to reach an acceptable estimate of the mean response as prescribed in NIST GCR 11-917-15 (2011). The synthetic accelerogram generation's primary purpose is to obtain a design acceleration time history with a response spectrum approximately matched to the target spectrum.

For the LRH analysis, Section 12.9 requires each component of ground motion to be spectrally matched over

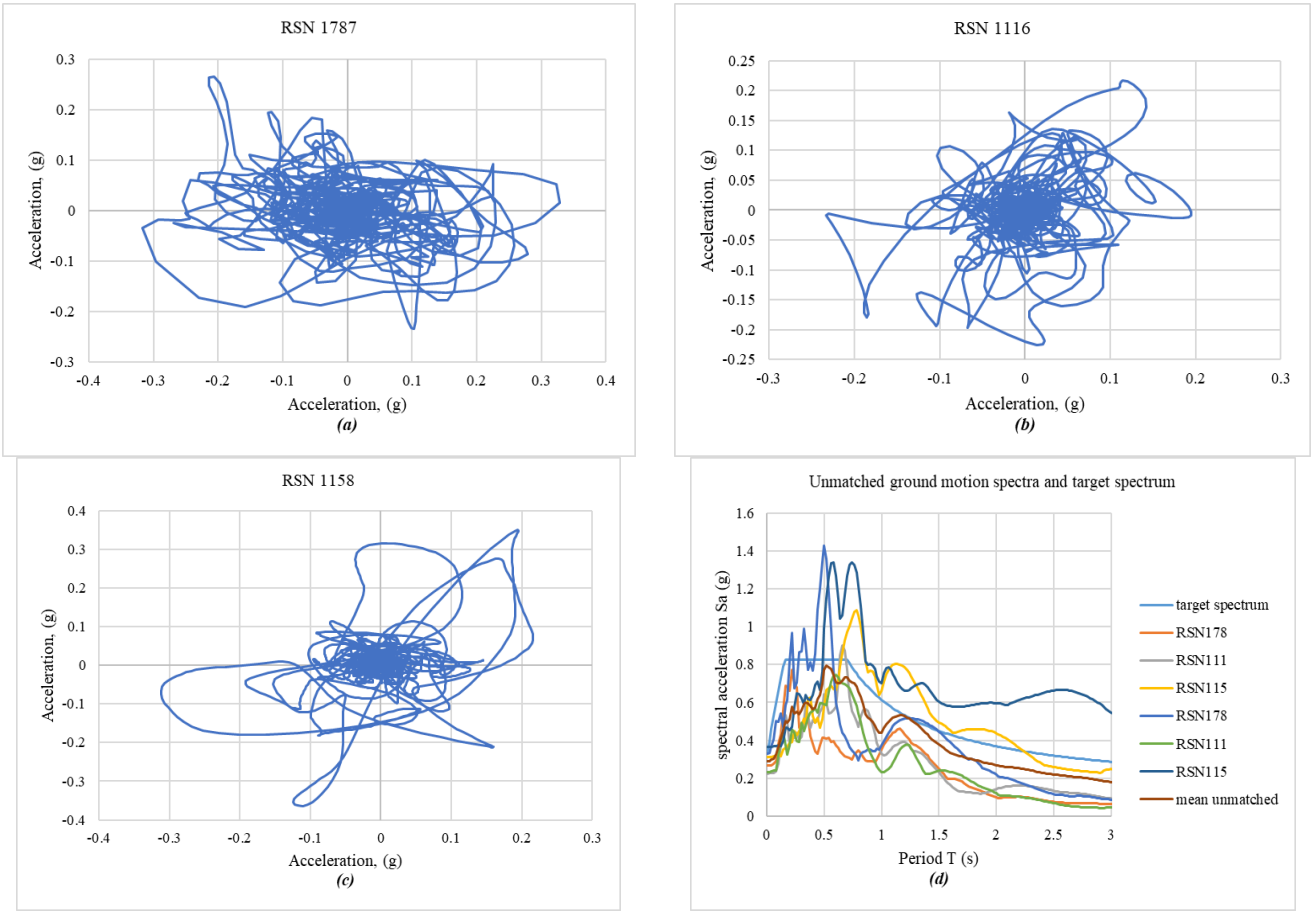

Fig. 4 (a), (b), (c) x- versus y-direction original ground acceleration, (d) unmatched ground motions, and target spectra

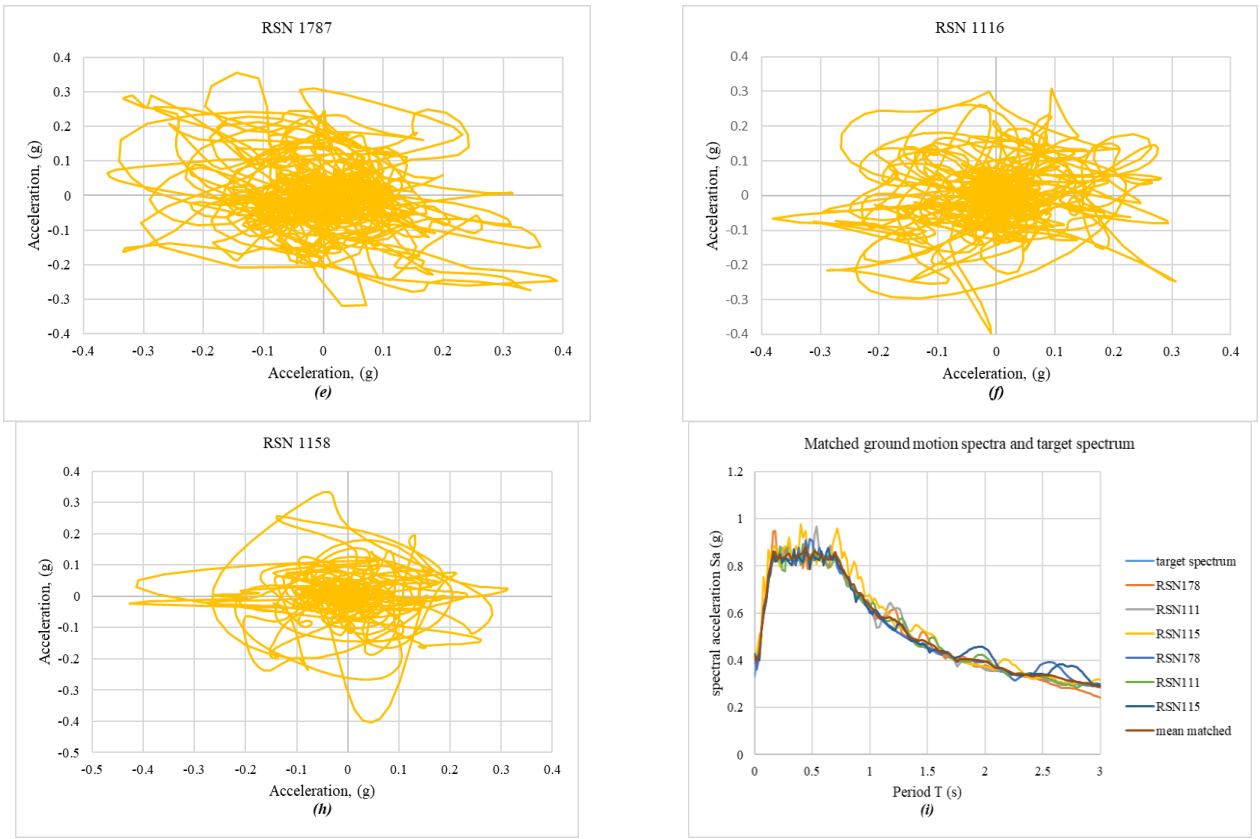

Fig. 5 (e), (f),(h) x- versus y-direction scaled ground acceleration, (i) matched ground motions and target spectra

Table 4 Modal properties

		Modal Participating Mass Ratios			Accumulated Modal Mass (%)		
Mode	Period(s)	UX	UY	RZ	Sum UX	Sum UY	Sum RZ
1	1.036	0.0071	0.672	0.0281	0.0071	0.672	0.0281
2	0.795	0.6219	0.0008	0.0726	0.629	0.6728	0.1007
3	0.715	0.0652	0.0396	0.592	0.6942	0.7124	0.6927
4	0.298	0.0002	0.0901	0.0024	0.6944	0.8026	0.6952
5	0.257	0.0341	0.0001	0.0051	0.7285	0.8026	0.7003
6	0.234	0.0001	0.062	0.0075	0.7286	0.8647	0.7078
7	0.226	0.0038	0.0093	0.0067	0.7325	0.8739	0.7145
8	0.179	0.1391	0.0001	0.001	0.8716	0.874	0.7155
9	0.164	0.0053	0.0046	0.1511	0.8769	0.8786	0.8666
10	0.119	0.0001	0.0602	0.0032	0.877	**0.9388**	0.8698
11	0.092	0.0672	0.0004	0.0035	**0.9443**	0.9392	0.8733
12	0.078	0.0001	0.0113	0.0057	0.9443	0.9504	0.879
13	0.073	0.0087	0.0135	0.0115	0.953	0.964	0.8904
14	0.073	0.002	0.0007	0.0428	0.955	0.9647	**0.9332**

the period range of 0.8 T_{lower} to 1.2·T_{upper}, where T_{lower} is the period at which 90% of the effective mass is captured, and Tupper is the fundamental period in the direction of response. For each direction of response and over the same period range, the mean of the 5% damped acceleration ordinates calculated employing the spectrum matched records should be at most 10% higher or lower than the target spectrum. The computer programs SesimoSignal and SeismoMatch by Seismosoft (2020) were used to perform signal processing and spectral matchings. They are capable of matching over a period range of interest with a predefined tolerance (Bozorgnia *et al.* 2014). For this study, the indicated period range for the spectral matching was between 0.05 and 3, and the input tolerance was equal to 0.3. Two horizontal components of matched ground acceleration in x- versus y-direction are plotted in (e), (f), and (h) of Fig. 5(i) represents the target spectrum used for the MRS and LRH analysis, and three pairs of matched ground motion spectra.

3. Results and discussion

The effective modal mass ratio is a measure of each mode's contribution to the total base shear. It can be used in order to define how many modes we need to take into account. In the case study, the sum of effective modal mass ratios are represented in Table 4 as accumulated modal mass expressed as a percentage. The response of all modes of vibration contributing significantly to the global response should be taken into account. The sum of the effective modal masses for the modes taken into account amounts to at least 90% of the structure's total mass. It is suitable to consider all modes with participating mass greater than 5%. The adequate number of modes that capture nearly 90% of the modal mass participation is shown in bold in Table 4. The three first modes' modal participation factors are 0.672, 0.629, and 0.6927 and indicate that the first and second modes are related to lateral translation in Y- and X-direction with periods 1.036 and 0.795, respectively. The third mode is related to rotation around Z-direction with a period of 0.715s. Besides, it is noticeable that the extracted fundamental periods from ETABS are considerably higher than the empirical period used in ELF analysis, which is C_uT_a=0.66.

Due to regularity in plan and elevation of the case study RC building, the higher mode effects may not be very influential. As shown in Table 4 and C_uT_a the empirical period is lower than those of the analytical one. This is because the effect of infill walls, staircases, nonstructural elements, and other elements that affect the lateral stiffness of the structure is neglected in the analytical model. Also, EI modifiers assumption for out-of-plane and in-plane stiffness of shell element used for shear walls, which is 0.1 and 0.35, may produce an overly flexible analytical model. This is the case also for EI modifiers assumption for beams, columns and roof elements.

According to Section 12.8 of ASCE 7-16, drift is the inelastic displacement difference between two adjacent floors, which is the function of the Risk Category and structure's type and must not exceed the allowable drift limits (D_a) provided in Section 12.12 (Al-sheikh 2019). Accidental torsion requirements account for unconsidered mass distributions, uncertainties associated with stiffness, strength, and ground excitation. The eccentricity or distance between the center of mass and stiffness must be 5% of the building's width perpendicular to the applied loading. Torsional irregularity exists if the maximum story drift, including accidental torsion, at one end of the diaphragm or slab is more than 1.2 times the story drifts average at the edges of the diaphragm. Extreme torsional irregularity exists if one end of the diaphragm is more than 1.4 times the story's average drift at the edges of the diaphragm or slab and is not allowed for structures categorized in medium to high seismicity regions or SDC of E and F (Johnson 2015). The building's lateral force resisting system under consideration is dual in two orthogonal directions, and the stiffness is provided by RC moment-resisting frames and the RC shear walls. According to Section 12.12, the allowable story drift ratio for each response's direction is

Table 5 Drifts Ratios and Torsional Irregularity checking for X and Y direction loading

Story-Direction	D_{max}/h	D_{avg}/h	Ratio = D_{max}/D_{avg}	Ratio > 1.2	Torsional Irregularity?
7-X (Attic)	0.0100	0.0095	1.049	NO	NO
7-Y (Attic)	0.0108	0.0101	1.068	NO	NO
6-X (Roof)	0.0107	0.0104	1.028	NO	NO
6-Y (Roof)	0.0146	0.0126	1.156	NO	NO
5-X	0.0113	0.0109	1.028	NO	NO
5-Y	0.0159	0.0138	1.152	NO	NO
4-X	0.0116	0.0112	1.032	NO	NO
4-Y	0.0170	0.0148	1.146	NO	NO
3-X	0.0110	0.0105	1.039	NO	NO
3-Y	0.0166	0.0145	1.141	NO	NO
2-X	0.0087	0.0083	1.045	NO	NO
2-Y	0.0133	0.0117	1.132	NO	NO
1-X	0.0039	0.0036	1.070	NO	NO
1-Y	0.0041	0.0036	1.131	NO	NO

Table 6 Stability Analysis

Story-Direction	P_{total} (tonf)	V_{story} (tonf)	$D_{avg}I/hC_d$	stability index (θ)	$\theta_{max}= 0.5/\beta C_d \leq 0.25$	Okay?
7-X (Attic)	78.53	7.29	0.0020	0.021	0.1	OK
7-Y (Attic)	78.53	7.29	0.0027	0.029	0.1	OK
6-X (Roof)	792.51	66.45	0.0022	0.026	0.1	OK
6-Y (Roof)	792.51	66.45	0.0034	0.041	0.1	OK
5-X	1615.44	126.9	0.0024	0.031	0.1	OK
5-Y	1615.44	126.9	0.0037	0.047	0.1	OK
4-X	2438.36	175.34	0.0024	0.033	0.1	OK
4-Y	2438.36	175.34	0.0040	0.056	0.1	OK
3-X	3261.29	211.76	0.0023	0.035	0.1	OK
3-Y	3261.29	211.76	0.0039	0.060	0.1	OK
2-X	4084.51	236.17	0.0018	0.031	0.1	OK
2-Y	4084.51	236.17	0.0032	0.055	0.1	OK
1-X	4965.50	249.32	0.0008	0.016	0.1	OK
1-Y	4965.50	249.32	0.0014	0.028	0.1	OK

0.015, and owing to the sufficient structure's lateral stiffness, Drift ratios are within the acceptable range as is shown in Table 5.

According to Section 12.8, P-Delta effects may not be considered in structural analysis when the story stability index $\theta = (P\_x\ \Delta I_e)/(V\_x\ h_s\ x\ C_d) \leq 0.1$. If θ is between 0.1 and the stability index limit, $\theta_{max}=0.5/(\beta C_d) \leq 0.25$, all computed member forces and displacements from the first-order analysis should be increased by $1/(1-\theta)$ alternatively, the P–Δ analysis must be carried out. The term β is the ratio of shear demand to shear capacity for the story between levels x and x – 1, and usually is greater than one. Conservative code permitted β to be taken as 1.0. Where θ is greater than θ_{max}, the structure is potentially unstable and must be modified and redesigned. θ_{max} is less than 0.1 for cases in which $\beta = 1$ and C_d is greater than 5.0. The stability analysis using the ELF procedure is illustrated in Table 6, and as it can be seen, stability indices are below the maximum allowable limit.

According to chapter 22 of ACI 318-19, reduced nominal sectional strength should be greater or equal to factored load combination effects, for example, for bending moments $\varphi M_n = \varphi A_s F_y 0.9d \geq M_u$, where φ is the strength-reduction factor (Moehle 2017). According to chapter 18 of ACI 318-19 for the SMFs, members and joints shear forces are calculated considering probable bending moment $M_{pr} = As1.25F_y0.9d$ at both members ends, in addition to gravity load effects. The Capacity Design method should be used for the SMFs to ensure plastic hinges' formation in beams rather than columns (Park and Paulay 1975).

The total base shear and story shear distribution are compared for the three analysis methods in x- and y-direction responses. The story shear's envelope is illustrated in Fig. 6 using maximum absolute values of negative or positive responses between all load combinations. Generally, the calculated base shear using the ELF procedure is more conservative than the LRH and MRS methods. The mathematical structural model's eigenvalue analysis provided a significantly greater period due to mass and stiffness inaccuracies and neglecting stiffening effects of non-structural and architectural components and resulted in unconservative design base shear. Therefore, whether the extracted fundamental period of structure from an eigenvalue analysis is higher than the empirical period limit C_uT_a, the lower value between them should be utilized for design purposes. The empirical period limit is formulated

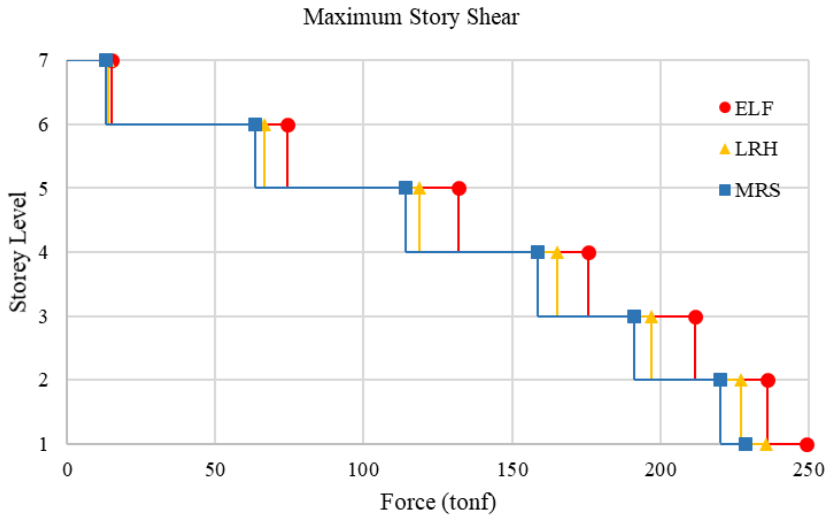

Fig. 6 Story Shear Comparisons

based on the lower bound of the period's data set, so it provides a lower bound estimate of a building's period with a given height and prevents using unconservative base shear from an excessively flexible mathematical structural model.

The vertical distribution of the ELF procedure's seismic forces is just a function of the exponent k and is expected to estimate the higher mode's effect. The exponent k is just a function of the structure's fundamental period; however, the building's actual first mode shape is also a function of the lateral force-resisting system's type. The vertical distributions for k=1 is a straight line, and if k=2, a parabola with its vertex at the base. The k=1 is suitable for buildings with a fundamental vibration period of 0.5 s or less, and k=2 is for buildings with a fundamental period of vibration of 2.5 s or higher. Section C12.8 presents a linear variation of k between 0.5s and 2.5 s fundamental period. The ELF lateral force distribution's accuracy is enhanced in buildings with the minor irregularity of stiffness and mass in plan and elevation.

The lateral force's distribution of the MRS method over the height is the superposition of several natural vibration modes. The contributions of vibration modes to the total base shear depend on the natural periods of vibration, response spectrum's shape, and modes shape that depend on the distribution of mass and stiffness over the height. Generally, for most irregular and tall structures, dynamic analysis approaches resulted in a more realistic distribution of inertial forces in the structure and reduced base shear concerning the ELF procedure. In LRH analysis, a mathematical structural model's response to actual recorded, simulated, or artificial earthquake records is defined by numerical integration of motion equations and provides a time-dependent history of the structure's response, and consider effects such as damping and provides information on the structure's stress and deformation during the time-history. LRH analysis preserves the signs of component forces, displacements, and reactions compared with MRS approach, in which the signs are lost due to the modal combination rules; however, it shows the maximum response quantities. It should be noted that this research's findings may not be a general trend, and further study and experiments are needed for various structures and methodologies.

Chopra (2017) implemented the MRS and LRH approach for a five-story shear frame. The MRS method's peak base shear estimated by the SRSS rule is smaller than the RHA values by approximately 10%. This value was around 15% for the top-story shear as the higher modes' responses are most significant relative to the first mode. Aswegan and Charney (2014) performed four different analysis of a four-story steel special moment frame building, and the results were compared. Their outcomes demonstrated that three spectral matched LRH cases provide base shears nearly 94% of MRS base shear using the ASCE 7-10 response spectrum. Inter-story drift ratios are a mean of 100% of the MRS inter-story drift ratios.

4. Conclusions

A comparative study of the three most popular methods of seismic analysis, Equivalent Lateral Force (ELF) method, Modal Response Spectrum (MRS) analysis, and Linear Response History (LRH) analysis has been carried out in this work using ETABS® software according to ASCE 7-16 standard. The three approaches have been examined in terms of story forces and base shear by analyzing a sixth-story reinforced concrete (RC) building. The calculation results in the present work for a building under consideration have shown that the ELF procedure's base shear is higher than those from the MRS or LRH analysis. According to Section 12.9 of the ASCE 7-16 standard, the MRS and LRH analysis require the scaling of forces to provide a conservative estimate of design base shear since the structure's fundamental period from an eigenvalue analysis may be higher than the standard's empirical period. The present study has shown that vertical distribution of the ELF procedure is only a function of the structure's fundamental period, and this method is limited for buildings with a uniform distribution of stiffness and

mass over the height and negligible torsional response. When higher-mode contributions are significant, the ELF method may neither be conservative nor accurately predict seismic forces' vertical distribution. On the other hand, this study has shown that MRS and LRH analyses preferentially define how the distribution of stiffness and mass of a structure influences the member forces and elastic displacements, while the LRH analysis preserves the signs of computed quantities lost in the modal combination rules and could be used as an alternative to the MRS analysis.

References

Abrahamson, N. (1992), "Non-stationary spectral matching", *Seismol. Res*. **63**, 30. https://doi.org/10.1785/gssrl.63.1.19

Ademović, N., Hadzima-Nyarko, M. and Zagora, N. (2020), "Seismic vulnerability assessment of masonry buildings in Banja Luka and Sarajevo (Bosnia and Herzegovina) using the macroseismic model", *Bull. Earthq. Eng*., **18**(8), 3897-3933. https://doi.org/10.1007/s10518-020-00846-8.

Al-sheikh, A. (2019), "ASCE 7-16 Provisions for Lateral Drift Determination", *Structure*, https://www.structuremag.org/?p=14696.

Al Atik, L. and Abrahamson, N. (2010), "An Improved Method for Nonstationary Spectral Matching", *Earthq. Spectra*, **26**(3), 601-617. https://doi.org/10.1193/1.3459159.

Applied Technology Council (ATC), "ATC Hazards by Location", https://hazards.atcouncil.org/

ASCE/SEI 7-16 (2017), *Minimum Design Loads and Associated Criteria for Buildings and Other Structures*.

Aswegan, K. and Charney, F.A. (2014), "A Simple Linear Response History Analysis Procedure for Building Codes", *Proceedings of the Tenth U.S. National Conference on Earthquake Engineering*, Anchorage, Alaska, July.

ATC (1978), Tentative Provisions for the Development of Seismic Regulations for Buildings, Report No. ATC3 ATC3-06, Applied Technology Council, Redwood City, U.S.A.

Bilgin, H. and Uruçi, R. (2018), "Effects of structural irregularities on low and mid-rise RC building response", *Chall. J. Struct. Mech.*, **4**(2) 33-44. https://doi.org/10.20528/cjsmec.2018.02.001

Bozorgnia, Y., Abrahamson, N.A., Atik, L.A., Ancheta, T.D., Atkinson, G.M., Baker, J.W. and Youngs, R. (2014), "NGA-West2 Research Project", *Earthq. Spectra*, **30**(3), 973-987. https://doi.org/10.1193/072113EQS209M.

Bulajić, B.Đ., Todorovska, M.I., Manić, M.I. and Trifunac, M.D. (2020), "Structural health monitoring study of the ZOIL building using earthquake records", *Soil Dyn. Earthq. Eng*., **133**, 1-35. https://doi.org/10.1016/j.soildyn.2020.106105.

Charney, F.A., Heausler, T.F. and Marshall, J.D. (2020), "Seismic Loads: Guide to the Seismic Load Provisions of ASCE 7-16", American Society of Civil Engineers, Reston, Virginia, U.S.A.

Chopra, A.K. (2017), *Dynamics of Structures: Theory and Applications to Earthquake Engineering*, Pearson Education, London, United Kingdom.

CSA A23.3 (2014), Standards Council of Canada - Conseil canadien des normes, Ottawa, Canada. https://www.scc.ca/en/standardsdb/standards/27660

Da Luo, D., Ning, C. and Li, B. (2019), "Effective torsional stiffness of reinforced concrete structural walls", *Earthq. Struct*., **16**(2), 119-127. https://doi.org/10.12989/eas.2019.16.2.000.

ETABS (2019), CSI (Computers and Structures Inc.), Walnut Creek, California.

Fajfar, P. (2018), "Analysis in seismic provisions for buildings: past, present and future", *Bull. Earthq. Eng*., **16**(7), 2567-2608. https://doi.org/10.1007/s10518-017-0290-8.

FEMA (1997), *NEHRP Guidelines for the Seismic Rehabilitation of Buildings, FEMA 273*, Applied Technology Council, Redwood City, U.S.A.

FEMA E-74 (2012), *Reducing the Risks of Nonstructural Earthquake Damage – A Practical Guide*, Applied Technology Council, Redwood City, U.S.A.

FEMA P-2082-1 (2020), *NEHRP Recommended Seismic Provisions for New Buildings and Other Structures, Volume I: Part 1 Provisions, Part 2 Commentary, Building Seismic Safety,* Council of the National Institute of Building Sciences, Washington, D.C., U.S.A.

FEMA P-58-2 (2008), *Seismic Performance Assessment of Buildings*, Applied Technology Council, Redwood City, U.S.A.

FEMA P695 (2009), *Quantification of Building Seismic Performance Factors*, Applied Technology Council, Redwood City, U.S.A.

Ghaemian, S., Muderrisoglu, Z. and Yazgan, U. (2020), "The effect of finite element modeling assumptions on collapse capacity of an RC frame building", *Earthq. Struct*., **18**(5), 555-565. http://dx.doi.org/10.12989/EAS.2020.18.5.555.

Ghosh, S.K. (2016), "Special reinforced concrete shear walls," *Structure,* https://www.structuremag.org/?p=10157.

Günay, S., Korolyk, M., Mar, D., Mosalam, K.M. and Rodgers, J. (2009), "Infill walls as a spine to enhance the seismic performance of non-ductile reinforced concrete frames", *Proceedings of the ATC and SEI Conference on Improving the Seismic Performance of Existing Buildings and Other Structures*, San Francisco, California, United States, December. https://doi.org/10.1061/41084(364)100.

Hadzima-Nyarko, M., Nikić, D. and Pavić, G. (2019), "Seismic vulnerability assessment of reinforced concrete frame structure by finite element analysis", *Acta Physica Polonica A*, **135**(4), 845-848. https://doi.org/10.12693/APhysPolA.135.845.

Hancock, J., Watson-Lamprey, J., Abrahamson, N.A., Bommer, J.J., Markatis, A., Mccoyh, E. and Mendis, R. (2006), "An improved method of matching response spectra of recorded earthquake ground motion using wavelets", *J. Earthq. Eng*., **10**, 67-89. https://doi.org/10.1080/13632460609350629.

Haselton, C.B., Baker, J.W., Stewart, J.P., Whittaker, A.S., Luco, N., Fry, A. and Pekelnicky, R.G. (2017), "Response history analysis for the design of new buildings in the NEHRP provisions and ASCE/SEI 7 standard: Part I - overview and specification of ground motions", *Earthq. Spectra*, **33**(2), 373-395. https://doi.org/10.1193/032114EQS039M.

Head, M., Dennis, S., Muthukumar, S., Nielson, B. and Mackie, K. (2014), "Nonlinear analysis in modern earthquake engineering practice", *Structure,* https://www.structuremag.org/?p=1666.

Heausler, T.F. (2015), "The most common errors in seismic design", *Structure,* https://www.structuremag.org/?p=8972.

Isik, E., Aydin, M.C. and Buyuksarac, A. (2020), "24 January 2020 Sivrice (Elazig) earthquake damages and determination of earthquake parameters in the region", *Earthq. Struct*., **19**(2), 145-156. http://dx.doi.org/10.12989/eas.2020.19.2.145.

Johnson, J.G. (2015), "Extreme torsional irregularity", *Structure,* https://www.structuremag.org/?p=8173.

Kanai, K. and Yoshizawa, S. (1963), "Some new problems of seismic vibrations of a structure. Part 1", *Bull. Earthq. Res. Inst*., **41**, 825-833.

Latifi, R. and Rouhi, R. (2020a), "Seismic assessment and retrofitting of existing RC structures: Seismostruct and Seismobuild implementation", *Civil Eng. Architect*., **8**(2), 84-93. https://doi.org/10.13189/cea.2020.080206.

Latifi, R. and Rouhi, R. (2020b), "Three-dimensional numerical model for seismic analysis of structures", *Civil Eng. Architect.*, **8**(3), 237-245. https://doi.org/10.13189/cea.2020.080306.

Li, B. and Mosalam, K.M. (2013), "Seismic performance of

reinforced-concrete stairways during the 2008 Wenchuan earthquake", *J. Perform. Constr. Facil.*, **27**(6), 721-730. https://doi.org/10.1061/(ASCE)CF.1943-5509.0000382.

Mindlin, R.D. (1951), "Influence of rotatory inertia and shear on flexural motions of isotropic elastic", *ASME J. Appl. Mech.*, **18**(1), 31-38.

Moehle, J. (2017), *Seismic Design of Reinforced Concrete Buildings*, McGraw Hill.

Moehle, J.P. and Alarcon, L.F. (1986), "Seismic analysis methods for irregular buildings", *J. Struct. Eng.*, **112**(1), 35-52. https://doi.org/10.1061/(ASCE)0733-9445(1986)112:1(35).

Moehle, J.P., Hooper, J.D., Kelly, D.J. and Meyer, T.R. (2010), "Seismic design of cast-in-place concrete diaphragms, chords, and collectors", NEHRP Seismic Design Technical Brief No. 3, produced by the NEHRP Consultants Joint Venture, a partnership of the ATC and the Consortium of Universities for Research in Earthquake Engineering, for the National Institute of Standards and Technology, Gaithersburg, MD.

NIST GCR 11-917-15 (2011), *Selecting and Scaling Earthquake Ground Motions for Performing Response-History Analyses*, National Institute of Standards and Technology, U.S.A.

NZS 3101 (2021), *Concrete Structures Standard*, Concrete Design Committee P 3101 for the Standards Council established under the Standards Act 1988. https://www.standards.govt.nz/sponsored-standards/building-standards/nzs3101-1-and-2/.

Park, R. and Paulay, T. (1975), *Reinforced Concrete Structures*. Wiley.

Rahmani, M. and Todorovska, M.I. (2013), "1D system identification of buildings during earthquakes by seismic interferometry with waveform inversion of impulse responses-method and application to Millikan library", *Soil Dyn. Earthq. Eng.*, **47**, 157-174. https://doi.org/10.1016/j.soildyn.2012.09.014.

Rahmani, M. and Todorovska, M.I. (2015), "Structural health monitoring of a 54-story steel frame building using a wave method and earthquake records", *Earthq. Spectra*, **31**(1), 501-525. DOI 10.1193/112912EQS339M.

Reddy, J.N. (2017), *Energy Principles and Variational Methods in Applied Mechanics*, Wiley.

Reissner, E. (1945), "The effect of shear deformation on the bending of elastic plates", *ASME J. Appl. Mech.*, **12**, A68-A77.

Seismosoft (2020), SeismoMatch 2020 - A computer program for Response Spectrum Matching. http://seismosoft.com/

Shehu, R., Angjeliu, G. and Bilgin, H. (2019), "A simple approach for the design of ductile earthquake-resisting frame structures counting for P-Delta effect", *Buildings*, **9**, 216. https://doi.org/10.3390/buildings9100216.

Snieder, R. and Safak, E. (2006), "Extracting the building response using seismic interferometry: theory and application to the Millikan Library in Pasadena, California", *Bull. Seism. Soc. Am.*, **96**(2), 586-598. https://doi.org/10.1785/0120050109.

Stewart, J.P., Abrahamson, N.A., Atkinson, G.M., Baker, J.W., Boore, D.M., Bozorgnia, Y. and Sabol, T.A. (2011), "Representation of bidirectional ground motions for design spectra in building codes," *Earthq. Spectra*, **27**(3), 927-937. https://doi.org/10.1193/1.3608001.

Strukar, K., Kalman Sipos, T., Jelec, M. and Hadzima-Nyarko, M. (2019), "Efficient damage assessment for selected earthquake records based on spectral matching", *Earthq. Struct.*, **17(**3), 271-282. https://dx.doi.org/10.12989/eas.2019.17.3.271

Timoshenko, S. (1959), *Theory of Plates and Shells*, McGraw-Hill.

Trifunac, M.D., Todorovska, M.I., Manić, M.I. and Bulajić, B.Đ. (2010), "Variability of the fixed-base and soil–structure system frequencies of a building-The case of Borik-2 building", *Struct. Control Heal. Monit.*, **17**(2), 120-151. https://doi.org/10.1002/stc.277.

Uang, C. and Maarouf, A. (1994), "Deflection Amplification Factor for Seismic Design Provisions", *J. Struct. Eng.*, **120**(8), 2423-2436. https://doi.org/10.1061/(ASCE)0733-9445(1994)120:8(2423).

Ugalde, D. and Lopez-Garcia, D. (2017), "Behavior of reinforced concrete shear wall buildings subjected to large earthquakes", *Procedia Eng.*, **199**, 3582-3587. https://doi.org/10.1016/j.proeng.2017.09.524.

Vintzileou, E., Zeris, C. and Repapis, C. (2004), "Seismic Behaviour of Existing RC Buildings", Paper No. 2453, *Proceedings of the 13th World Conference on Earthquake Engineering*, Vancouver, August. https://www.iitk.ac.in/nicee/wcee/article/13_2453.pdf.

Wong, J.M., Sommer, A., Briggs, K. and Ergin, C. (2017), "Effective Stiffness for Modeling Reinforced Concrete Structures", *Structure,* https://www.structuremag.org/?p=10924.

DK